Am J Cancer Res 2026;16(5):2025-2039
www.ajcr.us /ISSN:2156-6976/ajcr0171780

Original Article

BANF1 knockdown impedes thyroid cancer development and boosts CD8$^+$ T cell activity through PI3K/AKT/mTOR pathway

Chuanbing Liu*, Zhen Jia*, Dan Wei, Huanjun Wang

*Department of Endocrinology and Metabolism, The First Affiliated Hospital of Shandong First Medical University and Shandong Provincial Qianfoshan Hospital, Shandong Institute of Nephrology, Jinan, Shandong, China. *Equal contributors.*

Received January 29, 2026; Accepted May 18, 2026; Epub May 25, 2026; Published May 30, 2026

Abstract: Barrier to Autointegration Factor 1 (BANF1) is a highly evolutionarily conserved small DNA-binding protein, and its dysregulation has been implicated in the development of various diseases. This study seeks to elucidate the role of BANF1 in thyroid cancer and its relevance to tumor immunity. BANF1 expression levels were assessed using Western blot and RT-qPCR. The effects of BANF1 on thyroid cancer cell progression were evaluated using colony formation assays, EdU, Transwell migration/invasion assays, and Flow cytometry (FCM). The effects of BANF1 knockdown on CD8$^+$ T cell viability and cytokine secretion were examined using CCK-8 and FCM assays. Furthermore, the influence of BANF1 on proteins associated with the phosphatidylinositol 3-kinase/protein kinase B/mammalian target of rapamycin (PI3K/AKT/mTOR) pathway was detected. Our results showed that BANF1 expression was significantly higher in thyroid cancer tissues compared with the adjacent tissues. BANF1 inhibition induced apoptosis and suppressed the proliferative, migratory, and invasive potential of thyroid cancer cells. However, BANF1 knockdown had no significant effect on the growth of transplanted tumors in BALB/c immunodeficient nude mice Moreover, inhibition of BANF1 enhanced CD8$^+$ T cell proliferation and cytokine production. Mechanistically, BANF1 knockdown promoted activation of the PI3K/AKT/mTOR pathway. In summary, BANF1 knockdown suppresses thyroid cancer cell progression and enhances CD8$^+$ T cell vitality, potentially through modulating the PI3K/AKT/mTOR signaling pathway in CD8$^+$ T cells.

Keywords: BANF1, thyroid cancer, expression, malignant progression, CD8$^+$ T cells

Introduction

Thyroid cancer, a common malignant tumor of the endocrine system, is pathologically classified into several subtypes based on its histopathological characteristics: papillary carcinoma, follicular adenocarcinoma, medullary carcinoma, and undifferentiated carcinoma [1]. The overall 5-year survival rate of thyroid cancer is approximately 90%; however, its incidence has been increasing annually in most countries, including China, the United States, Canada, and G20 nations [2]. The development of thyroid cancer is attributed to multiple factors, including genetic and epigenetic genetic variations, as well as environmental factors. Early symptoms of thyroid cancer often resemble those of benign thyroid diseases. Clinically, it frequently presents as an asymptomatic neck mass, which may lead to overlooking the possibility of malignancy and delayed diagnosis [3]. In clinical practice, surgical intervention remains the primary treatment for thyroid cancer. Postoperative management may require adjunctive therapies, including endocrine therapy, immunotherapy, or radioisotope therapy, depending on disease progression [4, 5]. Therefore, identifying novel biomarkers that can effectively diagnose thyroid cancer is crucial for the treatment.

Barrier to Autointegration Factor 1 (BANF1) is a DNA-binding protein that links DNA to nuclear envelope-associated structural proteins [6]. BANF1 is involved in multiple biological processes, including nuclear assembly, mitosis,

https://doi.org/10.62347/SOAT5677

chromatin organization, gene regulation, and DNA damage response, and has been implicated in tumor progression [7]. Previous studies have demonstrated that BANF1 expression is related to recurrence-free survival in breast cancer patients [8]. Inactivating BANF1 demonstrates tumor-suppressive effects by reducing the proliferative, migratory, and invasive capacities of gastric cancer cells [9]. Furthermore, BANF1 regulates colorectal cancer progression via modulating GLI1 activity [10]. However, the specific mechanisms by which BANF1 contributes to thyroid cancer development remain unclear and require further investigation.

The tumor immune microenvironment plays a pivotal role in cancer initiation and progression. Tumor-infiltrating lymphocytes (TILs) exert distinct effects on tumor immune microenvironment and tumor development [11]. $CD8^+$ T cells, as a subgroup of T lymphocytes, are key mediators of antitumor immunity. They can directly kill tumor cells by releasing cytotoxic proteins such as granzyme and perforin, and indirectly induce tumor cell death via releasing tumor necrosis factor-alpha (TNF-α) and interferon-gamma (IFN-γ). In addition, $CD8^+$ T cells accelerate tumor cell apoptosis through the FAS-FASL signaling pathway [12]. Currently, dysfunction of $CD8^+$ T cells has been observed in a large number of tumor types [13].

This study investigated BANF1 expression in thyroid cancer. By knocking down BANF1 in 8505C and TPC-1 thyroid cancer cells, we examined its effects on cell proliferation, migration, invasion, and apoptosis. Subsequently, the regulatory effect of BANF1 on $CD8^+$ T cell activity was explored, aiming to provide a potential therapeutic target for thyroid cancer.

Materials and methods

Databases

The TIMER database (https://cistrome.shinyapps.io/timer) was utilized to analyze BANF1 expression in thyroid cancer. Furthermore, UALCAN database (https://ualcan.path.uab.edu/index.html) was utilized to analyze BANF1 expression across different thyroid cancer subtypes. Additionally, the GEPIA3 database (https://gepia3.bioinfoliu.com/) was employed to evaluate the association between BANF1 expression and overall survival (OS) and progression-free survival (PFS) in thyroid cancer patients.

Patient samples

A total of 48 patients with thyroid cancer admitted to our hospital were selected. Thyroid cancer tissues and paired adjacent normal tissues were collected, preserved in cryotubes and frozen at -80°C until further use. Inclusion criteria: (1) Histologically confirmed thyroid cancer; (2) Complete clinical and pathological data; (3) Age ≥18 years. Exclusion criteria: (1) History of other malignancies; (2) Prior radiotherapy or chemotherapy before surgery; (3) Incomplete clinical data or loss to follow-up; (4) Concurrent cardiac, hepatic, or renal dysfunction.

This study was approved by the Ethics Committee of The First Affiliated Hospital of Shandong First Medical University & Shandong Provincial Qianfoshan Hospital (No. (S625) [2024]), and all procedures were performed in accordance with the Declaration of Helsinki.

Cell culture

Thyroid cancer cell lines 8505C, KTC-1, B-CPAP and TPC-1 (TW-Reagent, Shanghai, China) were cultured in RPMI1640 medium (Abbkine, Wuhan, China). Cells were maintained in a humidified incubator at 37°C with 5% CO_2. Culture medium was refreshed every 24 hours to ensure optimal growth conditions.

Cell transfection

When cell confluency reached approximately 75%, transfection was performed. The transfection mixture, containing the target interference fragment and Lipofectamine 2000 (GIBCO, USA), was introduced into each well according to the manufacturer's instructions. After transfection, cells were returned to the incubator and cultured under standard conditions for subsequent experiments.

5-Ethynyl-2'-deoxyuridine (EdU)

A total of 4×10^3 cells were inoculated into 96-well plates and incubated at 37°C for 2 h with 100 μL EdU solution (Abbkine, Wuhan, China). Cells were fixed with 100 μL cell fixative (Beyotime, Shanghai, China) for 30 min. Then,

Table 1. Primer sequences used for RT-qPCR

Primer name	Sequence (5'-3')
BANF1-Forward	CTCCCAAAAGCACCGAGACT
BANF1-Reverse	CCCAGGACTTCACCAATCCC
GAPDH-Forward	TGTTCGTCATGGGTGTGAAC
GAPDH-Reverse	ATGGCATGGACTGTGGTCAT

100 μL Apollo reaction solution and 100 μL of 0.5% Triton X-100 were added. Finally, 100 μL Hoechst 33342 solution was added for DNA staining. Cell proliferation was observed and imaged under a microscope (Olympus Corporation, Japan).

Colony formation assay

Single-cell suspensions were inoculated into 6-well plates and cultured under normal conditions for 2-3 weeks until visible colonies formed. Cells were fixed with 4% paraformaldehyde (Beyotime, Shanghai, China) for 15 min and stained with 0.1% crystal violet (Beyotime, Shanghai, China). After cleaning and air-drying, images were captured, and the clone formation rate was calculated.

Reverse transcription quantitative polymerase chain reaction (RT-qPCR)

Total RNA was extracted from cell samples using cell lysis buffer and chloroform. Subsequently, cDNA synthesis using reverse transcription kit (TIANGEN, Beijing, China). Quantitative PCR was performed using the SYBR Green qPCR kit (Beyotime, Shanghai, China) with cDNA as the template. The reaction mixture consisted of 10 μL SYBR Green One, 2 μL DNA template, 0.5 μL of each forward and reverse primer, and 7 μL of ddH_2O. The qPCR program was as follows: initial denaturation at 95°C for 3 min, followed by 40 cycles of denaturation at 95°C for 5 s and annealing/extension at 60°C for 30 s. Relative expression of BANF1 was determined using the $2^{-\Delta\Delta CT}$ method, with GAPDH serving as the internal control gene. The primer sequences are detailed in **Table 1**.

Transwell assay

Cells in the logarithmic growth phase were digested and resuspended. Cell suspension (5×10^4 cells/mL) was added to the upper compartment of a Transwell insert, while 600 μL of cell culture medium were added to the lower chamber as a chemoattractant. After incubation for 24-48 h, migrated cells were fixed in 4% paraformaldehyde (Beyotime, Shanghai, China) at room temperature, stained, and observed under a microscope (Olympus Corporation, Japan). For the cell invasion assay, Transwell membranes were pre-coated with Matrigel, and the remaining procedures were identical to those of the cell migration assay.

Western blot

Cells were lysed by adding an appropriate volume of RIPA lysis buffer (Wanleibio, Shenyang, China), and total protein was collected following centrifugation. Protein concentration was determined using the BCA assay. Equal amounts of protein were separated by SDS-PAGE (Abbkine, Wuhan, China) and transferred onto polyvinylidene fluoride membranes (Elabscience, Wuhan, China). Membranes were sealed at room temperature for 1 h and the incubated overnight with primary antibodies. After washing, membranes were incubated with HRP-conjugated secondary antibodies at room temperature for 1 hour. Subsequently, protein bands were visualized using an enhanced chemiluminescence detection system. Primary antibodies used in this study included anti-GAPDH (1:1000, Cell Signaling Technology, USA), anti-BANF1 (1000, Abcam, UK), anti-PI3K (1:1000, Cell Signaling Technology, USA), anti-p-PI3K (1:1000, Cell Signaling Technology, USA), anti-AKT (1:1000, Cell Signaling Technology, USA), anti-p-AKT (1:2000, Cell Signaling Technology, USA), anti-mTOR (1:1000, Cell Signaling Technology, USA), anti-p-mTOR (1:1000, Cell Signaling Technology, USA). The secondary antibody was anti-rabbit IgG HRP-linked (1:1000, Cell Signaling Technology, USA).

Flow cytometry (FCM)

Cells from each experimental group were harvested and digested with trypsin (Pricella, Wuhan, China), followed by centrifugation at 4°C for 5 min. After discarding the supernatant, cells were resuspended in 500 μL 1× Binding Buffer. A 100 μL aliquot of the suspension was incubated with Annexin V-FITC and PI staining solution (E-CK-A211, Elabscience, Wuhan, China) for 15 min in the dark. Finally, 400 μL 1× Binding Buffer was added,

and samples were analyzed using a FACSCanto II flow cytometer (BD, USA).

Animal experiments

BALB/c nude mice were obtained from Hunan STA Laboratory Animal Co., Ltd. (Changsha, China). 8505C cells (1×10^7 cells/ml) were subcutaneously injected into the left axilla of the mice, with 5 mice per group. One to two weeks after injection, palpable solid masses were observed at the injection sites. Tumor volumes were measured on the 7th, 10th, 14st and 21th days after injection. On day 21, mice were euthanized using CO_2, and tumor tissues were excised for further analysis. All animal studies were approved by the Ethics Committee of The First Affiliated Hospital of Shandong First Medical University & Shandong Provincial Qianfoshan Hospital (No. (S583) [2024]).

Immunohistochemistry

The tumor tissues were sectioned and then subjected to baking, dewaxing, hydration and antigen repair. The slices were added to the 3% methanol and hydrogen peroxide (Solarbio, Beijing, China) blocking solution for 30 minutes. Incubation with primary antibody (1:200, Zenbio, Chengdu, China) was performed at 4°C overnight, followed by incubation with secondary antibody (1:500, Zenbio, Chengdu, China) at room temperature for 30 minutes. Then, DAB color development and hematoxylin (Beyotime, Shanghai, China) re-dyeing were carried out. After dehydration and transparency of the slices, the immunohistochemical results were interpreted under a microscope (Nikon eclipse 80i, Nikon, Japan).

Isolation of CD8+ T cells

Peripheral blood (10 mL) from thyroid cancer patients was centrifuged at 1,500 r/min for 10 min to separate plasma, which was then diluted with 30 mL PBS. 3 mL of diluted plasma was layered onto 15 mL human lymphocyte separation solution (Yuanye, Shanghai, China) and centrifuged at 2,500 rpm for 25 min. The mononuclear cell layer was collected, resuspended in 10 mL PBS, and centrifuged at 500 r/min for 10 min. The resulting pellet was resuspended in RPMI1640 medium to obtain peripheral blood mononuclear cells (PBMCs). PBMCs (1×10^7) were incubated with 20 μL CD8 magnetic beads in the dark for 20 min, and CD8+ T cells were isolated according to the manufacturer's instructions (Solarbio, Beijing, China). Subsequently, isolated CD8+ T cells were activated with CD3/CD28 magnetic bead (TL Biotechnology, Beijing, China) for 72 hours.

CD8+ T cell viability

CD8+ T cells were resuspended in acridine orange solution (Yita, Beijing, China) at a density of 1×10^6/mL and incubated in the dark for 10 min. Cells were then centrifuged for 5 min, and the supernatant was discarded. The cells were resuspended in PBS and photographed under a microscope (Nikon, Japan).

Statistical analysis

All experimental data were analyzed using SPSS 20.0 software. Data were expressed as mean ± standard deviation (SD). Homogeneity of variance was first tested for each dataset. Comparisons between two groups were performed using the unpaired Student's t-test. Comparisons among multiple groups were conducted using one-way ANOVA followed by Tukey's post hoc test. A p-value <0.05 was considered statistically significant.

Results

Expression of BANF1 in thyroid cancer tissues from databases

Analysis of TIMER2.0 database showed that BANF1 expression is significantly elevated in thyroid cancer tissues compared with adjacent normal tissues (**Figure 1A**). Similarly, the UALCAN database also demonstrated overexpression of BANF1 in thyroid cancer tissues (**Figure 1B**). Moreover, UALCAN database analysis indicated that BANF1 is highly expressed in all stages of thyroid cancer, with the highest level observed in stage IV (**Figure 1C**). Compared with normal tissues, BANF1 was significantly overexpressed in various histological subtypes of thyroid cancer (**Figure 1D**). Notably, BANF1 expression was relatively higher in patients with lymph node metastasis classified as N1 (**Figure 1E**).

BANF1 expression in clinical thyroid cancer samples

To verify the database findings, we further analyzed thyroid cancer tissues collected from

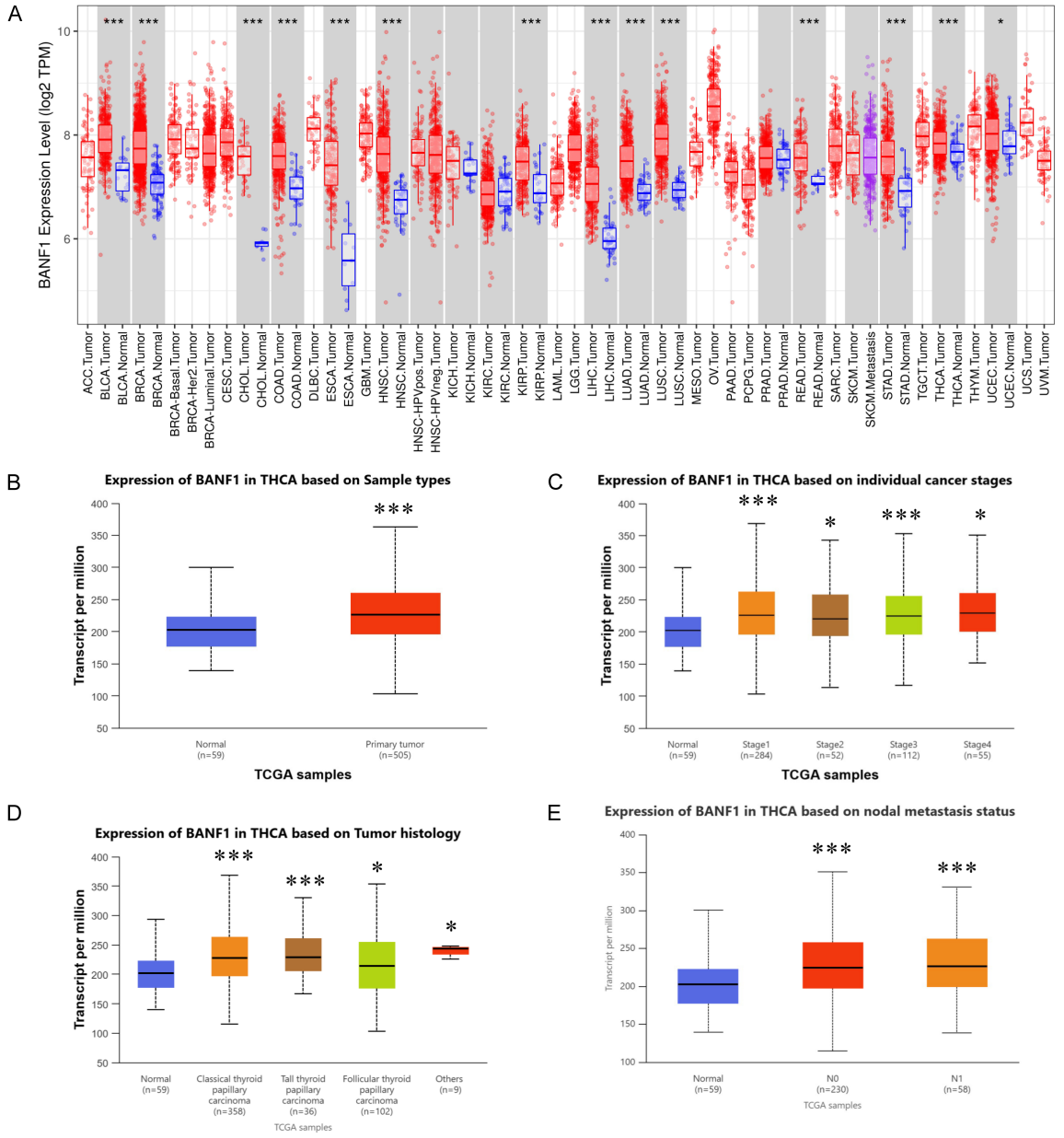

Figure 1. BANF1 expression is upregulated in thyroid cancer. A. BANF1 expression across various cancer types in the TIMER2.0 database; B. BANF1 expression in thyroid cancer tissues in UALCAN database; C. BANF1 expression in thyroid cancer at different stages; D. BANF1 expression in thyroid cancer based on tumor histology; E. BANF1 expression in thyroid cancer with different lymph node metastasis status. *P<0.05, ***P<0.001, compared to normal group. BANF1: barrier to autointegration factor 1.

our hospital. RT-qPCR and Western Blot analyses confirmed that BANF1 expression was significantly higher at both the mRNA and protein levels in tumor tissues compared to adjacent normal tissues (**Figure 2A**, **2B**). Meanwhile, IHC staining further demonstrated BANF1 upregulation in thyroid cancer tissues (**Figure 2C**). Collectively, these results consistently indicate that BANF1 is highly expressed in thyroid cancer, suggesting its potential role in the occurrence and development of thyroid cancer.

Clinical significance and prognostic value of BANF1 in thyroid cancer

Database analysis revealed no significant association between BANF1 expression and

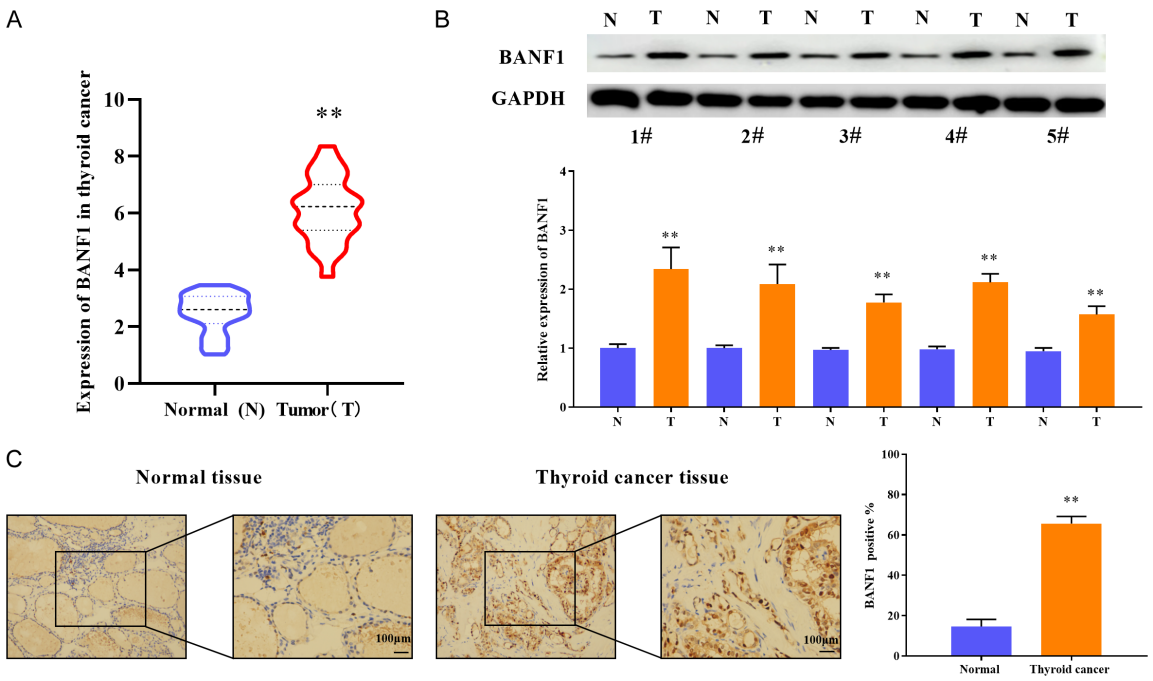

Figure 2. BANF1 expression in thyroid cancer tissue samples collected at our hospital. A. BANF1 mRNA expression analyzed by RT-qPCR; B. BANF1 protein expression detected by Western blot; C. IHC staining of BANF1 in thyroid cancer and adjacent normal tissues (100 μm, 100×). **P<0.01, compared to normal group. RT-qPCR: reverse transcription quantitative polymerase chain reaction; IHC: Immunohistochemistry.

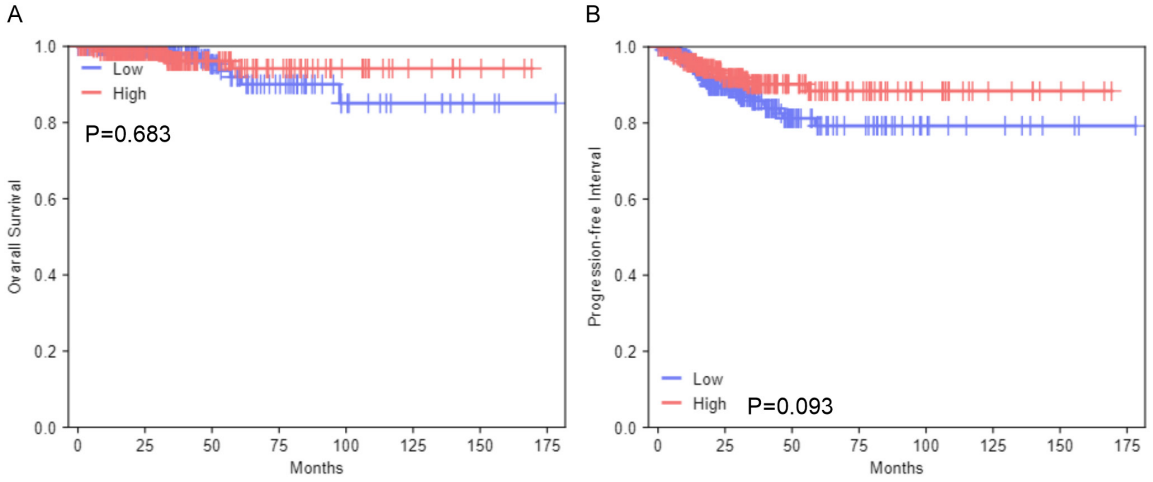

Figure 3. Correlation between BANF1 expression and survival outcomes in thyroid cancer patients. A. Association between BANF1 expression and overall survival of thyroid cancer patients; B. Association between BANF1 expression and progression-free survival of thyroid cancer patients.

either overall survival (OS) (**Figure 3A**) or progression-free survival (PFS) (**Figure 3B**) in thyroid cancer patients. However, the expression of BANF1 was substantially correlated with the clinical stage, multifocality, and lymph node metastasis (**Table 2**).

Inhibition of BANF1 expression suppressed the functions of thyroid cancer cells

Western blot analysis revealed elevated BANF1 expression in thyroid cancer cell lines (**Figure 4A**). BANF1 was knocked down in 8505C cells

Table 2. The relationship between BANF1 expression and clinicopathological characteristics of thyroid cancer patients

	n=48	High expression (n=24)	Low expression (n=24)	χ^2 value	*P* value
Age				0.375	0.540
≥55 years	16	9	7		
<55 years	32	15	17		
Tumor size				0.873	0.350
≥1 cm	15	6	9		
<1 cm	33	18	15		
Gender				0.505	0.477
Female	38	18	20		
Male	10	6	4		
Clinical stage				5.169	0.023
I + II	35	14	21		
III + IV	13	10	3		
Multifocality				5.689	0.017
Yes	18	13	5		
No	30	11	19		
Lymph node metastasis				4.090	0.043
Present	25	16	9		
Absent	23	8	15		

and TPC-1 cells (**Figure 4B**), and si-BANF1 2# was selected for subsequent functional assays. Knockdown of BANF1 significantly inhibited cell proliferation, as evidenced by EdU and colony formation assays (**Figure 4C**, **4D**), and increased apoptosis (**Figure 4E**). Moreover, the invasive and migratory capacities were also hindered by BANF1 knockdown (**Figure 4F**, **4G**). These findings indicate that BANF1 knockdown impedes the aggressive progression of thyroid cancer cells.

BANF1 knockdown prevented tumor growth in mice

Tumorigenesis assays were performed in BALB/c nude mice to evaluate the *in vivo* effects of BANF1. No significant differences in subcutaneous tumor volume were observed on days 7, 10, 14 and 21 post-injection between BANF1-knockdown and control groups (**Figure 5A**, **5B**). Immunohistochemical analysis revealed no significant differences in Ki67 or BANF1 positive rates between the two groups (**Figure 5C**). These findings suggest that BANF1 knockdown does not affect tumor growth in immunodeficient xenograft models, implying that BANF1 may exert its function by modulating immune cells rather than directly promoting tumor proliferation.

BANF1 knockdown enhanced the activity of CD8+ T cells

Under electron microscopy, CD8+ T cells displayed an elliptical shape and formed aggregates after cell expansion (**Figure 6A**). With the extension of culture time, CD8+ T cell viability increased gradually (**Figure 6B**). Subsequently, co-culture experiments were conducted using BANF1-depleted 8505C cells and CD8+ T cells, and the results showed that CD8+ T cell viability was enhanced (**Figure 6C**) and cell mortality rate was decreased (**Figure 6D**). In addition, expression levels of Ki67, INF-γ and GzmB in BANF1-knockdown group were elevated, while PD-1, Tim-3 and Caspase-3 were decreased compared to the control group (**Figure 6E**). These findings imply that BANF1 knockdown enhances CD8+ T cell activity.

BANF1 regulated CD8+ T cell activity via the PI3K/AKT/mTOR pathway

CD8+ T cells were treated with BANF1 knockdown, with or without the PI3K inhibitor LY-294002. BANF1 knockdown upregulated the

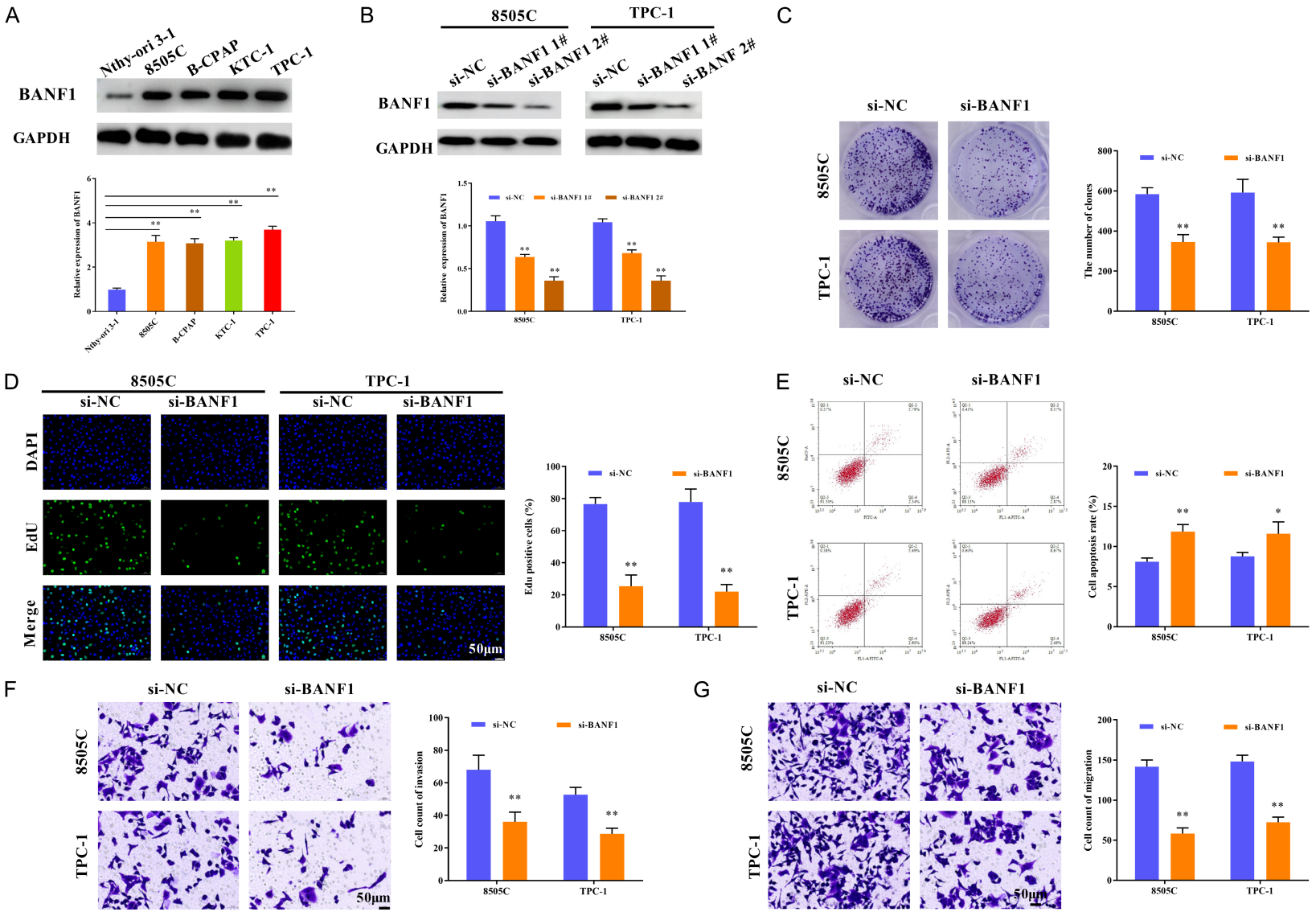

Figure 4. Effects of BANF1 knockdown on thyroid cancer cell viability. (A) Protein expression of BANF1 in thyroid cancer cells detected by Western blot; (B) Protein expression of BANF1 in 8505C and TPC-1 cells following si-BANF1 transfection; (C) Effects of BANF1 knockdown on cell proliferation assessed by EdU assay; (D) Effects of BANF1 knockdown on cell colony formation (50 μm, 200×); (E) Effects of BANF1 knockdown on cell apoptosis assessed by FCM method; (F, G) Effects of BANF1 knockdown on cell invasive (F) and migratory (G) capacities assessed by Transwell assay (50 μm, 200×). *P<0.05; **P<0.01, compared to si-NC group. EdU: 5-Ethynyl-2'-deoxyuridine; FCM: flow cytometry.

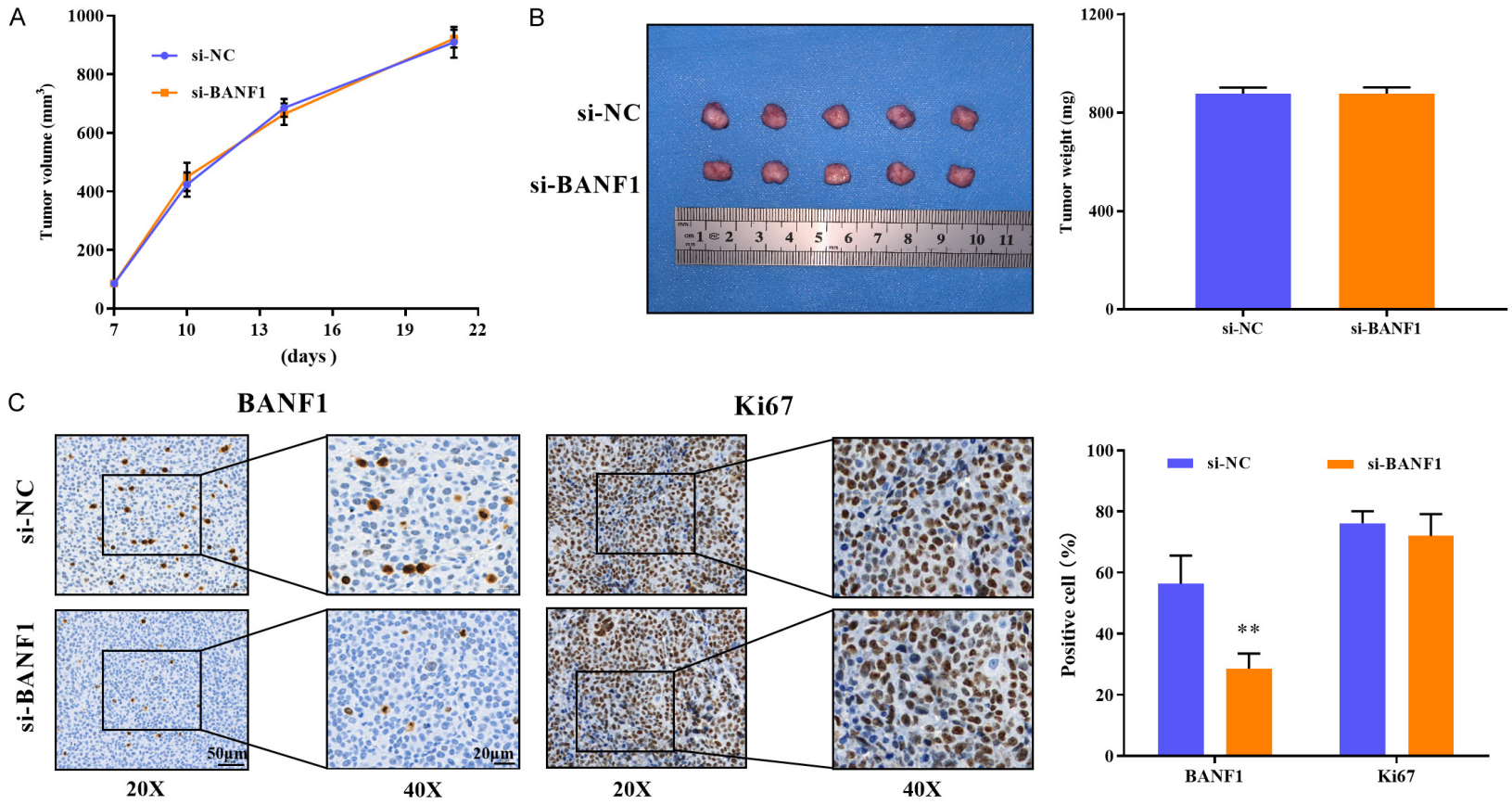

Figure 5. Effects of BANF1 knockdown on tumor growth in nude mice. A. Tumor volume after BANF1 knockdown; B. Comparison of tumor size and weight among groups at day 28; C. Immunohistochemical analysis showing the positive rates of BANF1 and Ki67 in tumor tissues (50 μm, 20×; 20 μm, 40×). **P<0.01, compared to si-NC group.

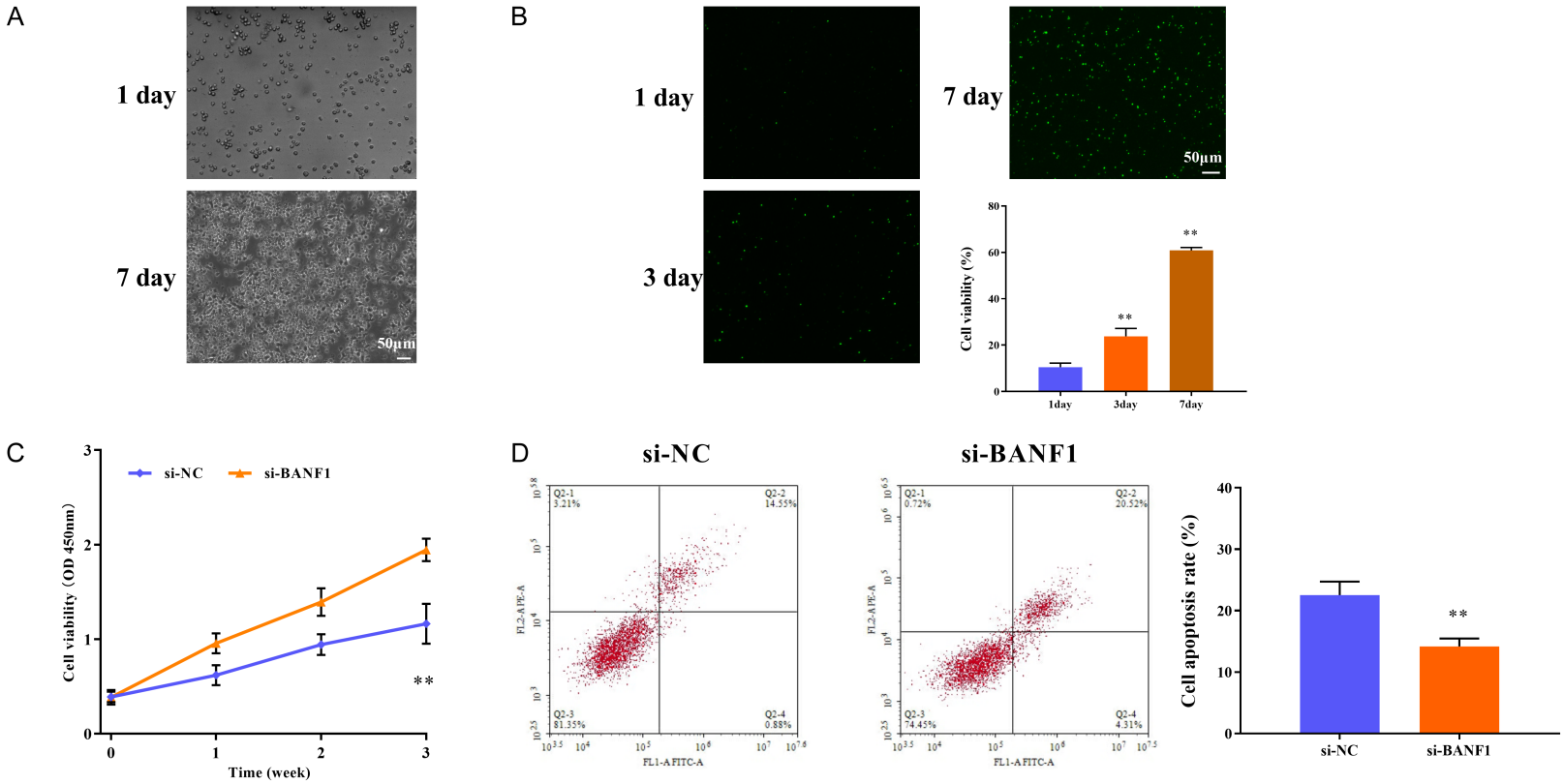
A
1 day
7 day
50μm
B
1 day
7 day
50μm
3 day
Cell viability (%)
1day
3day
7day
C
si-NC
si-BANF1
Cell viability (OD 450nm)
Time (week)
D
si-NC
si-BANF1
Q2-1
3.21%
Q2-2
14.55%
Q2-3
81.35%
Q2-4
0.88%
Q2-1
0.72%
Q2-2
20.52%
Q2-3
74.45%
Q2-4
4.31%
FL2-A:PE-A
FL1-A:FITC-A
Cell apoptosis rate (%)
si-NC
si-BANF1

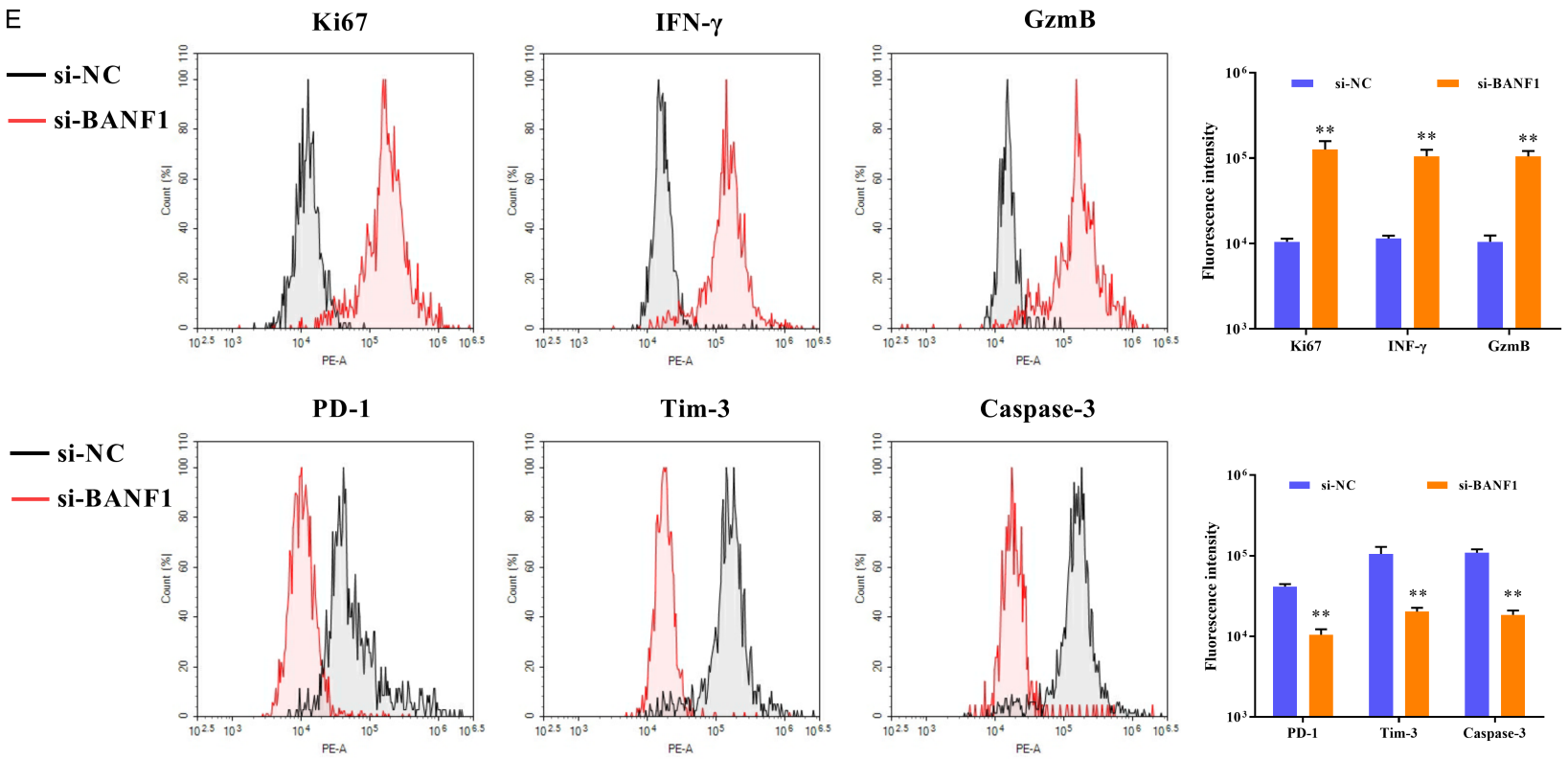

Figure 6. BANF1 knockdown enhanced CD8+ T cell activity. A. Morphology of CD8+ T cells under a microscope (50 μm, 200×); B. Viability of CD8+ T cells detected by acridine orange staining (50 μm, 200×); C. Effects of BANF1 knockdown on CD8+ T cell activity; D. Effects of BANF1 knockdown on CD8+ T cell apoptosis; E. Effects of BANF1 knockdown on cytokine levels in CD8+ T cells. **P<0.01, compared to si-NC group.

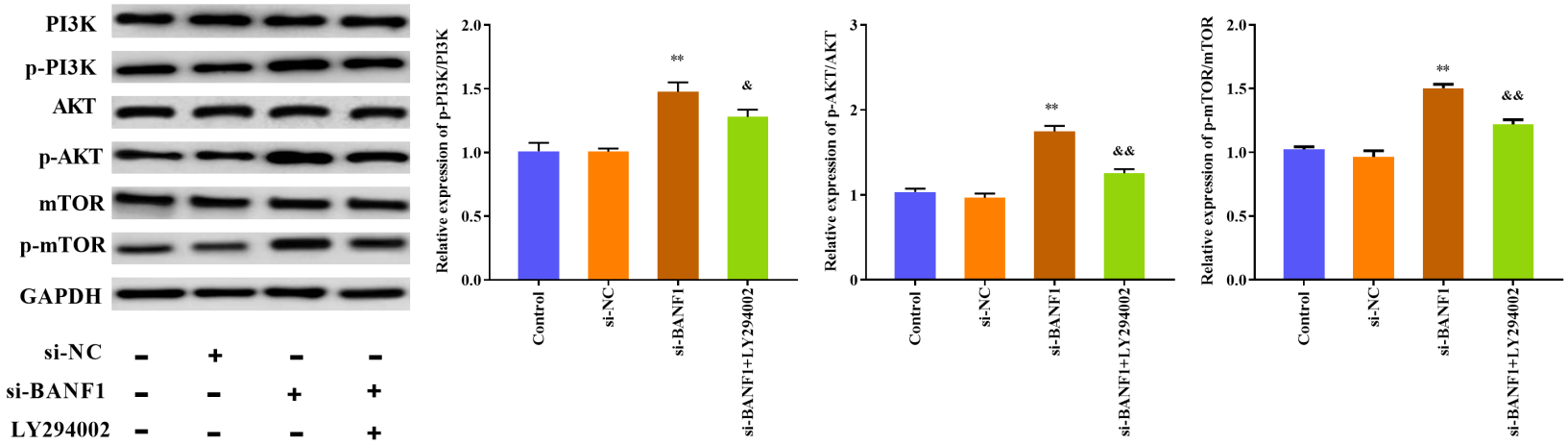

Figure 7. BANF1 regulates CD8+ T cell activity via the PI3K/AKT/mTOR pathway. &P<0.05, &&P<0.01, compared to si-BANF1 group; **P<0.01, compared to si-NC group. PI3K/AKT/mTOR: phosphatidylinositol 3-kinase/protein kinase B/mammalian target of rapamycin.

phosphorylation levels of PI3K, AKT and mTOR, while LY294002 reversed these effects (**Figure 7**). These findings indicate that BANF1 modulates CD8+ T cell activity through regulating the PI3K/AKT/mTOR pathway.

Discussion

Although timely surgical intervention generally results in a favorable prognosis for thyroid cancer patients, the incidence of this malignancy continues to rise rapidly [14]. Clinically, some patients still experience postoperative recurrence, refractory disease, and distant metastasis, which severely compromise survival outcomes [15]. Therefore, identifying novel molecular targets is crucial for the early diagnosis and prognostic assessment of thyroid cancer.

BANF1 localizes to the core region of the nucleus, where it recruits other nuclear membrane-anchoring and transmembrane proteins to facilitate nuclear envelope reorganization, a key step during cell mitosis [16, 17]. BANF1 plays a unique role in the tumorigenic progression of various malignancies [18]. For instance, in esophageal cancer, BANF1 expression is correlated with tumor differentiation and TNM stage [19]. BANF1 knockdown disrupts nuclear membrane integrity, induces mitosis arrest, and hinders cell proliferation, thus promoting selective cell death of breast cancer [20]. In this study, we observed elevated BANF1 expression in thyroid cancer tissues. Mechanistically, BANF1 knockdown suppressed thyroid cancer cell proliferation, migration, and invasion, while promoting apoptosis. These findings are consistent with previous reports in other malignancies, including cervical cancer cells [21] and head and neck squamous cell carcinoma [22]. Collectively, our results support that BANF1 functions as an oncogenic factor in thyroid cancer. However, we found that knockdown of BANF1 did not affect tumor growth in the immunodeficient xenograft model, suggesting that BANF1 may exert its effect by regulating immune cells.

CD8+ T cells, also known as cytotoxic T lymphocytes (CTLs), constitute a critical component of the heterogeneous population of tumor-infiltrating lymphocytes. They possess immunological memory and can rapidly differentiate into effector T cells upon reactivation, contributing to in anti-tumor immunity [23, 24]. Previous studies have shown that higher infiltration of CD8+ T cells in thyroid cancer is associated with longer overall survival [25], exerting protective effect in the context of thyroid cancer. It has been reported that BANF1 plays a pivotal role in modulating the antitumor immune response. Specifically, BANF1 knockdown activates the cGAS-STING pathway, thereby reducing the abundance of myeloid-derived suppressor cells and promoting CD8+ T cell infiltration [26]. Moreover, we found that BANF1 knockdown potentiated the activation of CD8+ T cells via the PI3K/AKT/mTOR pathway. Mechanistically, BANF1 deficiency or aberrant expression leads to nuclear envelope rupture and DNA damage [27], which triggers cellular stress responses including the activation of survival pathways such as PI3K/AKT/mTOR. Notably, prior research has shown that activation of the PI3K/mTOR/LDHA axis enhances glycolytic metabolism in CD8+ T cells, thereby sensitizing them to PD-1 immune checkpoint blockade [28]. Collectively, our results suggest that targeting BANF1 may potentiate anti-tumor immunity by modulating CD8+ T cell activity via the PI3K/AKT/mTOR pathway.

Several limitations of this study should be acknowledged. First, larger clinical cohorts with long-term follow-up are required to further validate the prognostic value of BANF1 in thyroid cancer. Second, although co-culture experiments demonstrated that BANF1 knockdown in thyroid cancer cells enhances CD8+ T cell activity, the specific molecular mechanisms underlying this intercellular communication remain to be fully elucidated. Third, the precise regulatory mechanisms by which BANF1 modulates the PI3K/AKT/mTOR signaling pathway warrant further investigation.

Conclusion

BANF1 knockdown inhibits the malignant progression of thyroid cancer cells, while simultaneously enhancing the activity of CD8+ T cells. Our findings highlight the oncogenic role of BANF1 in thyroid cancer and suggest that targeting BANF1 may represent a promising strategy for tumor immunotherapy.

Acknowledgements

This study was supported by Shandong Provincial Natural Science Foundation (No.

ZR2024MH270 and No. ZR2024MH190) and Bethune Foundation Thyroid Young and Middle-aged Program (No. Z04J2024E153).

Disclosure of conflict of interest

None.

Address correspondence to: Dan Wei and Huanjun Wang, Department of Endocrinology and Metabolism, The First Affiliated Hospital of Shandong First Medical University and Shandong Provincial Qianfoshan Hospital, Shandong Institute of Nephrology, Jinan, Shandong, China. E-mail: 77weidan@163.com (DW); wanghuanjun007@163.com (HJW)

References

[1] Voelker R. What is thyroid cancer? JAMA 2024; 332: 346.
[2] Gong Y, Jiang Q, Zhai M, Tang T and Liu S. Thyroid cancer trends in China and its comparative analysis with G20 countries: Projections for 2020-2040. J Glob Health 2024; 14: 04131.
[3] Forma A, Kłodnicka K, Pająk W, Flieger J, Teresińska B, Januszewski J and Baj J. Thyroid cancer: epidemiology, classification, risk factors, diagnostic and prognostic markers, and current treatment strategies. Int J Mol Sci 2025; 26: 5173.
[4] Boucai L, Zafereo M and Cabanillas ME. Thyroid cancer: a review. JAMA 2024; 331: 425-435.
[5] Cunha LL and Ward LS. Translating the immune microenvironment of thyroid cancer into clinical practice. Endocr Relat Cancer 2022; 29: R67-R83.
[6] Rose M, Bai B, Tang M, Cheong CM, Beard S, Burgess JT, Adams MN, O'Byrne KJ, Richard DJ, Gandhi NS and Bolderson E. The impact of rare human variants on barrier-to-auto-integration factor 1 (Banf1) structure and function. Front Cell Dev Biol 2021; 9: 775441.
[7] Jamin A and Wiebe MS. Barrier to autointegration factor (BANF1): interwoven roles in nuclear structure, genome integrity, innate immunity, stress responses and progeria. Curr Opin Cell Biol 2015; 34: 61-68.
[8] Zhang G. Expression and prognostic significance of BANF1 in triple-negative breast cancer. Cancer Manag Res 2020; 12: 145-150.
[9] Xu Y, Wang X, Yuan W, Zhang L, Chen W and Hu K. Identification of BANF1 as a novel prognostic biomarker in gastric cancer and validation via in-vitro and in-vivo experiments. Aging (Albany NY) 2024; 16: 1808-1828.
[10] Wang X, Xu Y, Chan S, Zhao H, Huang S, Wang Y, Yang Y, Wang Z, Zuo X, Zhang H and Chen W. VRK1/BANF1/GLI1 axis regulates tumor development and progression of colorectal cancer. Int J Biol Sci 2025; 21: 3144-3163.
[11] Lv B, Wang Y, Ma D, Cheng W, Liu J, Yong T, Chen H and Wang C. Immunotherapy: reshape the tumor immune microenvironment. Front Immunol 2022; 13: 844142.
[12] Peng S, Lin A, Jiang A, Zhang C, Zhang J, Cheng Q, Luo P and Bai Y. CTLs heterogeneity and plasticity: implications for cancer immunotherapy. Mol Cancer 2024; 23: 58.
[13] Philip M and Schietinger A. CD8(+) T cell differentiation and dysfunction in cancer. Nat Rev Immunol 2021; 22: 209-223.
[14] Reverter JL. Thyroid cancer. Med Clin (Barc) 2025; 164: 421-428.
[15] Schlumberger M and Leboulleux S. Current practice in patients with differentiated thyroid cancer. Nat Rev Endocrinol 2020; 17: 176-188.
[16] Duan T, Thyagarajan S, Amoiroglou A, Rogers GC and Geyer PK. Analysis of a rare progeria variant of Barrier-to-autointegration factor in Drosophila connects centromere function to tissue homeostasis. Cell Mol Life Sci 2023; 80: 73.
[17] Young AM, Gunn AL and Hatch EM. BAF facilitates interphase nuclear membrane repair through recruitment of nuclear transmembrane proteins. Mol Biol Cell 2020; 31: 1551-1560.
[18] Harb OA, Elfeky MA, Alabiad MA, Hemeda R, Allam AS, El Hawary AT, Elbaz M, Sharaf AL, Gertallah LM, Abdelaziz AM, Shalaby AM, Alorini M, Yahia AIO and Negm M. PYCR1, BANF1, and STARD8 expression in gastric carcinoma: a clinicopathologic, prognostic, and immunohistochemical study. Appl Immunohistochem Mol Morphol 2023; 32: 102-110.
[19] Li J, Wang T, Pei L, Jing J, Hu W, Sun T and Liu H. Expression of VRK1 and the downstream gene BANF1 in esophageal cancer. Biomed Pharmacother 2017; 89: 1086-1091.
[20] Rose M, Burgess JT, Cheong CM, Richard I, Suraweera A, Adams MN, Duijf PHG, O'Byrne KJ, Richard DJ and Bolderson E. The inner nuclear membrane protein, Banf1, has an essential role in triple negative breast cancer cell proliferation and survival. Sci Rep 2025; 15: 25492.
[21] Mao L, Zhang Y, Mo W, Yu Y and Lu H. BANF1 is downregulated by IRF1-regulated microRNA-203 in cervical cancer. PLoS One 2015; 10: e0117035.
[22] He Y, Li H, Li J, Huang J, Liu R, Yao Y, Hu Y, Yang X and Wei J. BANF1 is a novel prognostic biomarker linked to immune infiltration in head and neck squamous cell carcinoma. Front Immunol 2024; 15: 1465348.

[23] Chen Y, Yu D, Qian H, Shi Y and Tao Z. CD8(+) T cell-based cancer immunotherapy. J Transl Med 2024; 22: 394.
[24] Park J, Hsueh PC, Li Z and Ho PC. Microenvironment-driven metabolic adaptations guiding CD8(+) T cell anti-tumor immunity. Immunity 2023; 56: 32-42.
[25] Yang Z, Wei X, Pan Y, Xu J, Si Y, Min Z and Yu B. A new risk factor indicator for papillary thyroid cancer based on immune infiltration. Cell Death Dis 2021; 12: 51.
[26] Wang M, Huang Y, Chen M, Wang W, Wu F, Zhong T, Chen X, Wang F, Li Y, Yu J, Wu M and Chen D. Inhibition of tumor intrinsic BANF1 activates antitumor immune responses via cGAS-STING and enhances the efficacy of PD-1 blockade. J Immunother Cancer 2023; 11: e007035.
[27] Burgess JT, Cheong CM, Suraweera A, Sobanski T, Beard S, Dave K, Rose M, Boucher D, Croft LV, Adams MN, O'Byrne K, Richard DJ and Bolderson E. Barrier-to-autointegration-factor (Banf1) modulates DNA double-strand break repair pathway choice via regulation of DNA-dependent kinase (DNA-PK) activity. Nucleic Acids Res 2021; 49: 3294-3307.
[28] Liu T, Zeng F, Li Z, Cheng L, Yan X, Chen H, Liu Q, Li X, Li Z, Yao J, Xu D, Chen Z, Wang F, Wang J and Zhang J. Lypd6b depletion promotes CD8(+) T cell-mediated anti-tumor immunity via metabolic reprogramming in colorectal cancer. Nat Commun 2025; 17: 675.